Characteristics of a HSS-driven magnetic storm in the high-latitude ionosphere

N. Ellahouny, A. Aikio, M. Pedersen, H. Vanhamäki, I. Virtanen, J. Norberg, M. Grandin, Al.Kozlovsky, T. Raita, K. Kauristie, A. Marchaudon, P.-L. Blelly, S.-I. Oyama

1) Ionospheric Physics Research Unit, University of Oulu, Finland, 2) Finnish Meteorological Institute, Helsinki, 3) CoE in Sustainable Space, University of Helsinki 4) Sodankylä Geophysical Observatory, Finland, 5) IRAP, University of Tolouse, France,6) Institute for Space-Earth Environmental Research, Nagoya University, Nagoya, Japan

Email: Nada.Ellahouny@oulu.fi

UNIVERSITY OF OULU

1. Introduction

Solar wind high-speed streams (HSSs) >400 km/s that emanate from Solar coronal holes have a significant impact on the geomagnetic activity during the declining phase of the solar cycle [Gonzalez et al., 1999; Tsurutani et al.,2006]. When HSSs catch up the preceding slow solar wind, they create a compressed plasma region, called co-rotating interaction region (CIR). HSSs can induce geomagnetic storms that last for several days [Borovsky and Denton, 2006] and affect the ionospheric behavior, specially at the high latitudes [Grandin et al., 2015; Marchaudon et al., 2018]. When a magnetospheric substorm takes place, injection of electrons and protons occur. In this poster, we present one of the longest storms in the current solar cycle (24) that occurred on 14th of March 2016.

2. Data and initial results

2.1 Solar wind driver

Figure 1 is an image of the solar disc taken by (SDO/AIA). It shows coronal holes, which are the HSS origin. The HSSs can be seen in solar wind parameters in this event that lasts for 8 days as shown in **Figure 2.**

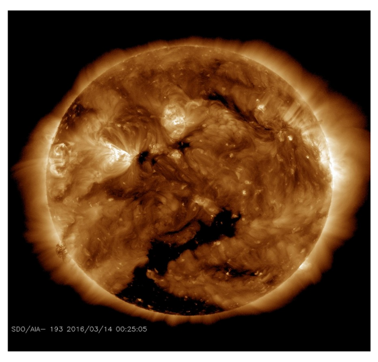

Figure 1 Solar wind flowing from the coronal hole (14 March 2016).

Solar wind bulk speed shows gradual increase from 370 to 560 km/s (**Figure 2a**) and the total magnetic field increases from 6 to 20 nT (**Figure 2b**) which flags the start of the storm (14 March 2016 17:20 UT) marked by the vertical solid line [Grandin et al., 2018]. Akasofu epsilon parameter (**Figure 2c**) is calculated, which gives an estimate of the energy input into the magnetosphere [Akasofu, 1979]. It reaches 1100 GW in the firststday of the storm (D1). Using selected magnetometers from IMAGE network, we calculated local electrojet IL and IU indices, shown in **Figure 2d, which** correspond to westward (WEJ) and eastward (EEJ) electrojets, respectively. The global auroral activity can be seen along with the local auroral activity in **Figure 2e** as AE and IE, respectively. The AE exceeds 1000 nT many times during the storm, while IE exceeds 800 nT many times as well. Dst index that is assumed to be a direct measure of ring current intensity and describes the evolution of the magnetic storm is displayed in **Figure 2f**. It reaches a minimum of -56 nT. The Kp index (not shown) reaches 5 that represents a minor magnetic storm (G1).

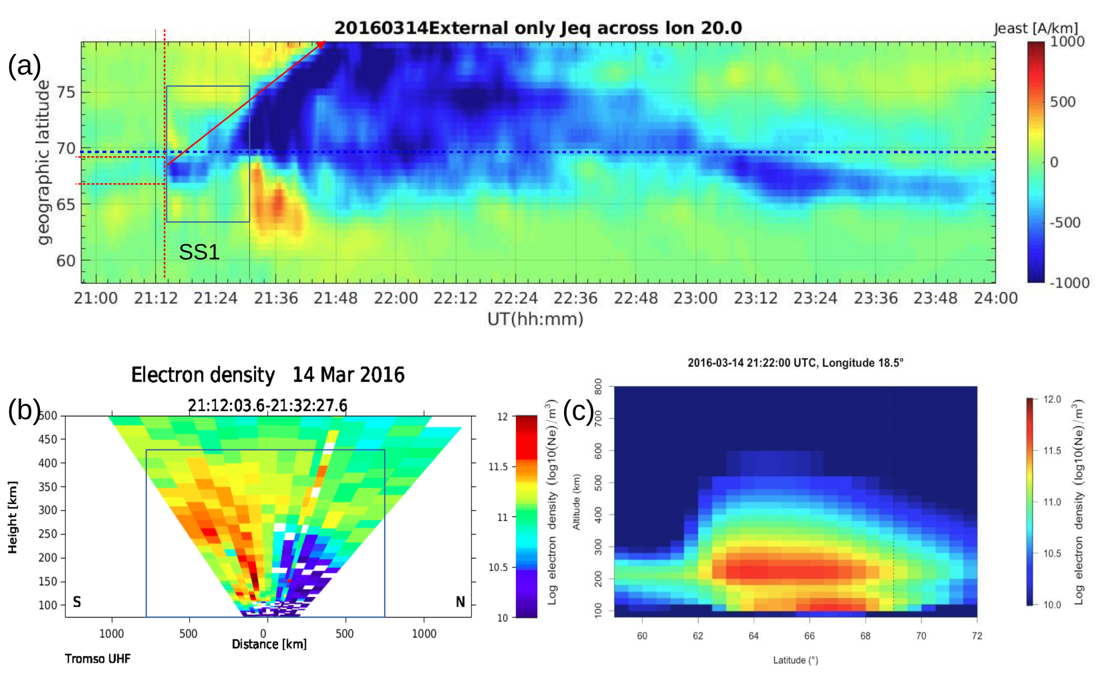

Figure 4 a) 1-D equivalent current during the 1st substorm (SS1), the horizontal blue dotted line indicates the location of Tromsø, the two dotted horizontal red lines indicate the latitudes width of the SS onset, the boxes bounds the time for the observation in the lower panel. b) the meridian scan of EISCAT radar for the electron density height profile, 0 correspondence to 69.6° Lat c) TomoScand electron density during the same time.

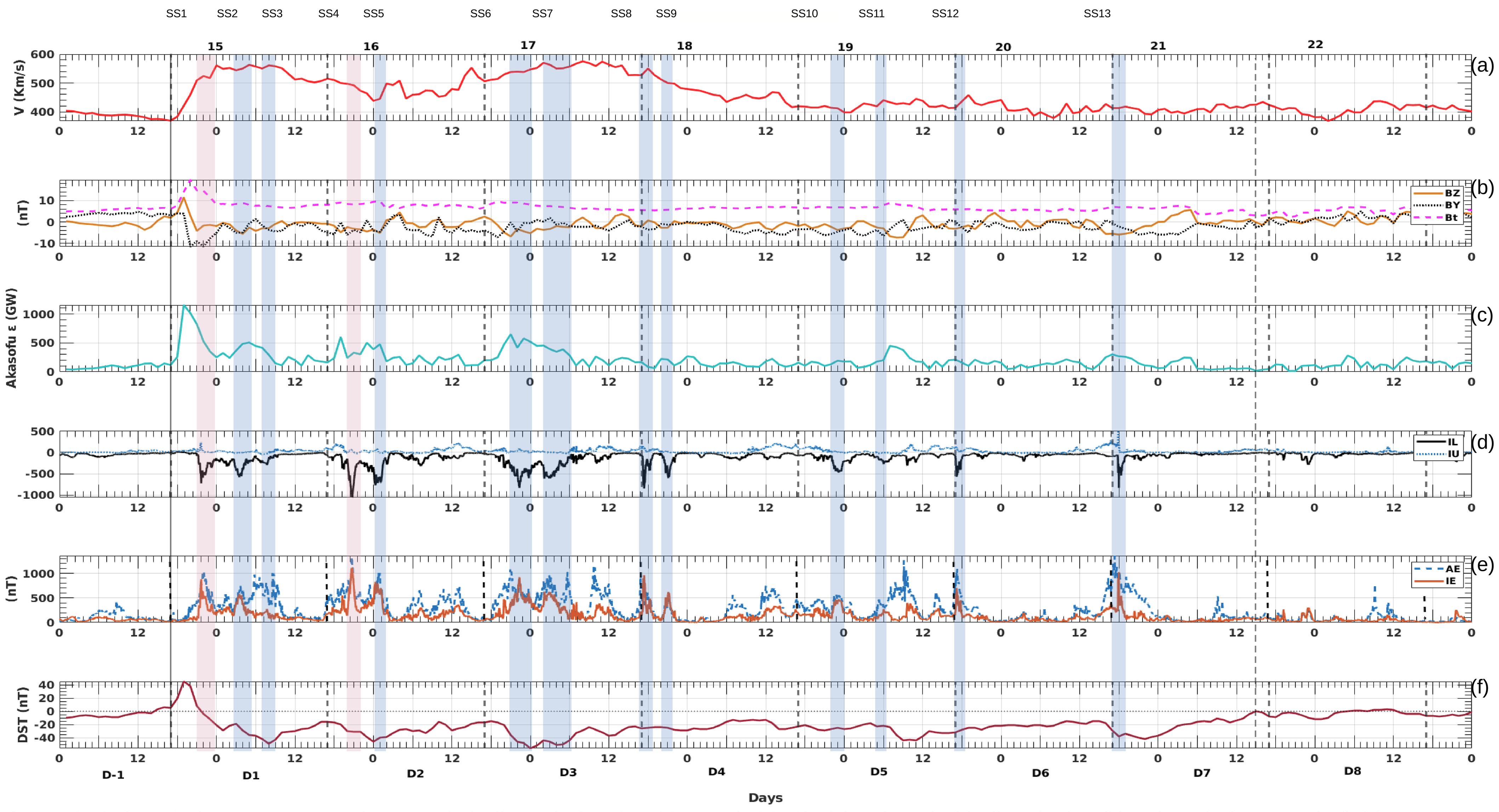

Figure 2 Solar wind parameters and magnetic indices during (14-22 March 2016). (a) solar wind bulk velocity, (b) solar wind magnetic field components (Bz,By,Bt), (c) Akasofu epsilon parameter,(d) local magnetic indices from IMAGE magnetometers (IU,IL), (e) the local (IE) and global (AE) electrojet indices, (f) Dst index. The shaded blue areas indicates the substorms during this event, the two red shaded areas are the candidates for our study.

2.2 Substorms

Using the 1-D equivalent currents plots generated from IMAGE magnetometers (examples shown in **Figure 4a, 5a)**, we identified 13 substorms (SS). SS onsets of expansion phases are identified by a sudden intensification and poleward expansion of the WEJ.

Figure 3 shows correlation between the SS onset latitude for midnight sector events and SYM-H, so that onsets take place at lower latitude when ring current is more intense.

In our study we show two examples of substorms (SS1 and SS4, red bars in **Figure 2**). We selected those, since they both occur during decreasing Dst, onset latitudes are roughly the same, and whose onsets take place in the midnight sector.

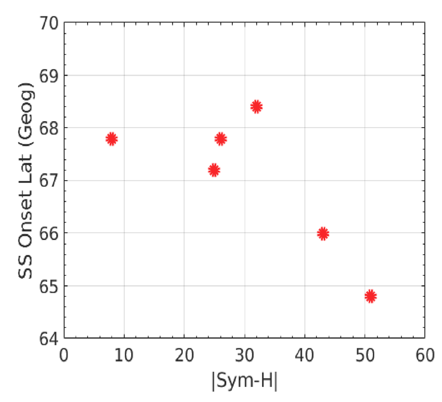

Figure 3 Midnight SS absolute Sym-H values during the minimum (IL) versus SS onset latitudes.

2.3 Cosmic Noise Absorbtion (CNA)

As a statistical study made by [Grandin et al., 2015], CNA is frequently seen during long events and extends to subauroral latitudes. Using two riometer stations (ABI, SOD) in **Figure 5d** we found during SS4 expansion and recovery phases a high value of ionospheric absorption (~3.2dB, the bounded box) in both stations, which is caused by electron density enhancement in the D region during precipitating energetic particles.

2.4 EISCAT data

Using EISCAT Tromsø data, we show ionospheric electron density during SS1 and SS4 (**Figure 4b, 5b, 5c**). In SS1 **Figure 4b** bounded box, we see E layer enhancement during the intensified (WEJ) over Figure 4a bounded box. During times of SS4 bounded boxes in **Figure 5a**, we detect E and D layer enhancement. That was in a good agreement with the CNA data.

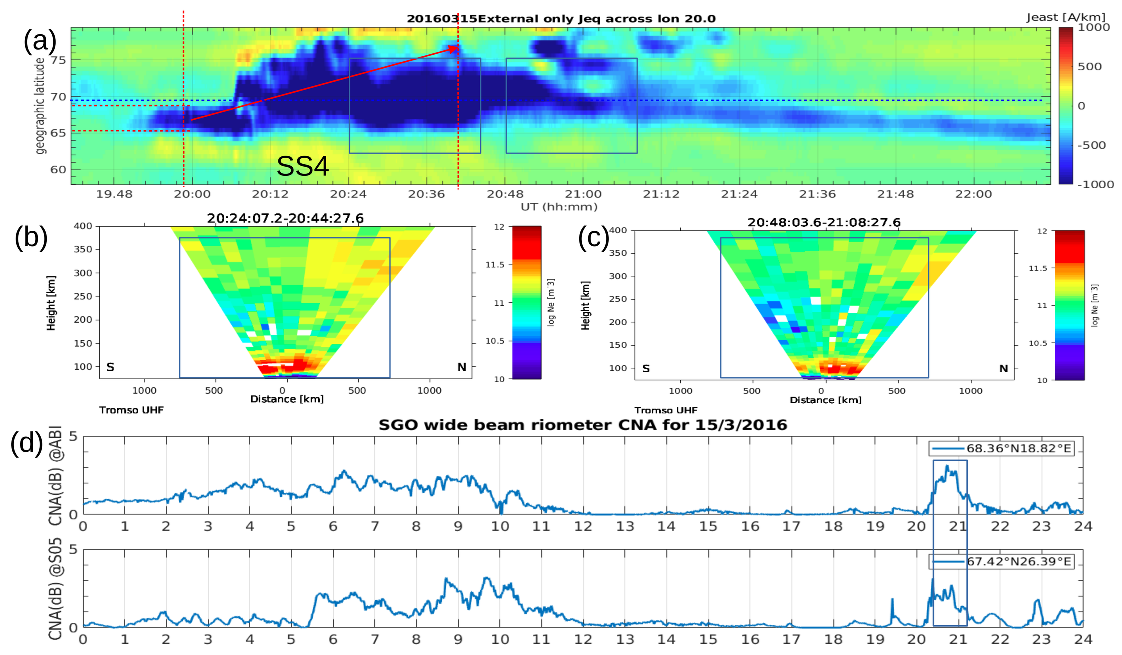

Figure 5 a) 1-D equivalent current during the 4th substorm (SS4), the horizontal blue dotted line indicates the location of Tromsø,the two dotted horizontal red lines indicates the latitudes width of the SS onset, the rectangle bounds the time for the observation in the middle panels. b) and c) are the meridian scans of EISCAT radar for the electron density height profile, d) CNA for Abisko and Sodankylä reiometers stations during 15 March 2016.

2.5 Tomoscand measurments

Tomoscand uses beacon and GNSS satellite data for 3-D ionospheric tomography. During SS1 bounded box in **Figure 4a, b**, Tomoscand electron densities are shown in **Figure 4c**. A perfect detection of E and F layer enhancement was observed in Tomoscand result along with the EISCAT Tromsø electron density measurements.

3. Future plans

The aim of this study is to look at ionospheric behavior on a time scale of several days during (HSS) forcing. In this event,we have a magnetic storm of 8 days, during which we have 13 substorms, affecting E- and D region electron densities.

In addition to substorms, we will study the F-region behavior (decreases in electron density) during the storm.

References

Akasofu, S.-I. (1979), A search for the interplanetary quantity controlling the development of geomagnetic storms, Q. J. R. Astron. Soc., 20,119–137.

Borovsky, J. E., and M. H. Denton (2006), Differences between CME-driven storms and CIR-driven storms, J. Geophys. Res., 111, A07S08, doi:10.1029/2005JA011447.

Gonzalez, W. D., B. T. Tsurutani, and A. L. Clúa de Gonzalez (1999), Interplanetary origin of geomagnetic storms, Space Sci. Rev., 88, 529–562, doi:10.1023/A:1005160129098.

Grandin, M., A. T. Aikio, A. Kozlovsky, T. Ulich, and T. Raita (2015), Effects of solar wind high-speed streams on the high-latitude ionosphere: Superposed epoch study, J. Geophys. Res. Space Physics, 120, 10,669–10,687, doi:10.1002/2015JA021785.

Grandin, M., Aikio, A. T., Kozlovsky, A., Ulich, T., & Raita, T. (2017). Cosmic radio noise absorption in the high□latitude ionosphere during solar wind high speed streams. Journal of Geophysical Research: Space Physics, 122(5), 5203-5223.

Marchaudon, A., Blelly, P. -L., Grandin, M., Aikio, A., Kozlovsky, A., & Virtanen, I. (2018). IPIM Modeling of the Ionospheric F-2 Layer Depletion at High Latitudes During a High-Speed Stream Event. Journal of geophysical research. Space physics, 123(8), 7051-7066. https://doi.org/10.1029/2018JA025744.

Tsurutani, B. T., et al. (2006), Corotating solar wind streams and recurrent geomagnetic activity: A review, J. Geophys. Res., 111, A07S01, doi:10.1029/2005JA011273.